

See discussions, stats, and author profiles for this publication at: <https://www.researchgate.net/publication/263955541>

HOI versus HOIO selectivity of a molten-type AgI electrode

ARTICLE in THE JOURNAL OF PHYSICAL CHEMISTRY A · JUNE 2014

Impact Factor: 2.69 · DOI: 10.1021/jp504052w

CITATION

1

READS

69

8 AUTHORS, INCLUDING:



[Zoltan Noszticzius](#)

Budapest University of Technology and Econo...

100 PUBLICATIONS 1,840 CITATIONS

SEE PROFILE



[Maria Wittmann](#)

Budapest University of Technology and Econo...

39 PUBLICATIONS 510 CITATIONS

SEE PROFILE



[Stanley Furrow](#)

Pennsylvania State University Berks College

32 PUBLICATIONS 483 CITATIONS

SEE PROFILE



[Guy Schmitz](#)

Université Libre de Bruxelles

77 PUBLICATIONS 546 CITATIONS

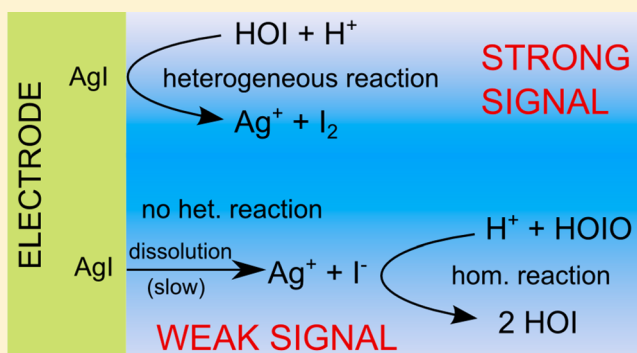
SEE PROFILE

HOI versus HOIO Selectivity of a Molten-type AgI Electrode

Gábor Holló,[†] Kristóf Kály-Kullai,[†] Thuy B. Lawson,[†] Zoltán Noszticzius,[†] Maria Wittmann,^{*,†} Norbert Muntean,^{‡,§} Stanley D. Furrow,[§] and Guy Schmitz^{||}[†]Department of Physics, Budapest University of Technology and Economics, H-1521 Budapest, Hungary[‡]Department of Physical Chemistry, Babes-Bolyai University, RO-400028 Cluj-Napoca, Romania[§]Penn State Berks College, The Pennsylvania State University, Reading, Pennsylvania 19610, United States^{||}Faculty of Applied Sciences, Université Libre de Bruxelles, CP165/63, Av. F. Roosevelt 50, 1050 Brussels, Belgium

S Supporting Information

ABSTRACT: AgI electrode is often applied not only to determine iodine concentration but also to follow oscillations in the weakly acidic medium of the Bray–Liebhafsky and Briggs–Rauscher reactions where it partly follows the hypoiodous acid (HOI) concentration. It is known that HOI attacks its matrix in the corrosion reaction: $\text{AgI} + \text{HOI} + \text{H}^+ \rightleftharpoons \text{Ag}^+ + \text{I}_2 + \text{H}_2\text{O}$ and the AgI electrode measures the silver ion concentration produced in that reaction. The signal of the electrode can be the basis of sensitive and selective HOI concentration measurements only supposing that an analogous corrosive reaction between AgI and iodic acid (HOIO) can be neglected. To prove that assumption, the authors calibrated a molten-type AgI electrode for I^- , Ag^+ , HOI, and HOIO in 1 M sulfuric acid and measured the electrode potential in the disproportionation of HOIO, which is relatively slow in that medium. Measured and simulated electrode potential versus time diagrams showed good agreement, assuming that the electrode potential is determined by the HOI concentration exclusively and the contribution of HOIO is negligible. An independent and more direct experiment was also performed giving the same result. HOIO was produced with a new improved recipe. Conclusion: an AgI electrode can be applied to measure the HOI concentration selectively above the so-called solubility limit potential.

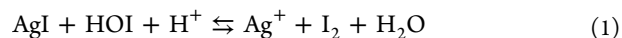


■ INTRODUCTION

The study of iodine speciation in waters is of great significance for the proper daily iodine intake by humans and for atmospheric pollution. Iodine exists in seawater, rain, and municipal water mainly as iodide, iodate and organic compounds. Molecular iodine is also formed by oxidation of iodide or reduction of iodate, and the hydrolysis of iodine produces hypoiodous acid ($\text{I}_2 + \text{H}_2\text{O} \rightleftharpoons \text{HOI} + \text{I}^- + \text{H}^+$), which in turn is an important intermediate in the formation of iodine organic compounds and has a particularly important role in the exchange of iodine between seawaters and the atmosphere.^{1–3} HOI is also a component of the waste streams from nuclear reactors.⁴ On the other hand, hypoiodous acid is a crucial intermediate in complex systems like the Bray–Liebhafsky (BL)^{5–14} and Briggs–Rauscher (BR)^{15–33} oscillating reactions. Kinetic studies and modeling of all these systems would benefit greatly from a sensitive device measuring the concentrations of HOI. Such a device was proposed recently³² as well as a new method to prepare HOI solutions.

We developed a new type of iodide selective electrode³² prepared by dipping silver wire into molten silver iodide. It was shown that the electrode (similarly to the traditional AgI pellet based iodide selective electrodes) responds not only to Ag^+ and I^- ions but is also sensitive to HOI above the so-called

solubility limit potential (SLP), where $[\text{I}^-] = [\text{Ag}^+] = (K_s)^{1/2}$ at the surface of the electrode (K_s is the solubility product of AgI). The Nernstian potential response of the electrode to HOI was explained by the corrosion potential theory.^{34,35} In accordance with that theory, HOI reacts with the AgI coating of the electrode to generate Ag^+ ions in the corrosion reaction in eq 1.



The electrode actually measures the steady-state Ag^+ ion concentration at its surface, which is established in reaction and diffusion processes of the various components. The Nernstian potential response is due to a linear relationship between the Ag^+ ion concentration at the surface of the electrode and the HOI concentration in the bulk.

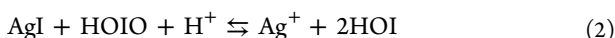
The important problem that we study in this work is the selectivity of such an electrode for HOI. An electrode potential above the SLP indicates that $[\text{Ag}^+] > (K_s)^{1/2}$ at the surface of the electrode. If no Ag^+ ions are present in the bulk then Ag^+ ions can only come from the electrode due to some corrosion process. In an acidic medium, three oxyiodine species

Received: April 25, 2014

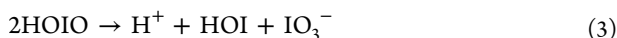
Revised: May 30, 2014

(neglecting the radical ones) might react with AgI and cause corrosion: I(+1) (HOI and/or its protonated form), I(+3) (HOIO, that is iodic acid and/or its protonated form) and I(+5) (IO_3^- and/or HOIO_2 , that is iodate and/or iodic acid).

Earlier experiments^{34,36} demonstrated that corrosion potentials due to I(+5) are negligible because the rate of the iodate–iodide reaction is much slower than the rate of the hypiodous acid–iodide reaction in the homogeneous phase and a heterogeneous corrosion reaction is probably even slower. (All corrosion processes should involve a heterogeneous step since one reaction partner, AgI, is in the solid, while the corrosive reactants are in the liquid phase.) However, a corrosion potential caused by I(+3) might be more significant. This is because the rate of the homogeneous $\text{HOIO} - \text{I}^-$ reaction is rather high (regarding its suggested rate constant³⁶ in a 1 M sulfuric acid medium it can be even faster than the $\text{HOI} - \text{I}^-$ reaction), thus we cannot exclude that the heterogeneous reaction, eq 2,



is also fast enough to give a corrosion signal. Actually, at least in theory, I(+3) could even give a stronger corrosion signal than HOI itself, if the rate constant of eq 2 was not much smaller than that of eq 1, as in eq 2 one HOIO produces two HOI molecules which can generate further corrosion. However, in a previous work, Noszticzius et al.³⁵ followed the disproportionation reaction, eq 3, of iodic acid:



with an iodide-selective electrode and found that the corrosion signal was rising during the process, which indicated that HOI gives a stronger corrosion signal than HOIO. Nevertheless, in that work HOI contamination in the calibrating HOIO solution prevented measurement of a corrosion signal exclusively due to iodic acid and, as a first approximation, it was assumed to be zero.

In the present work, to study the question of the HOI versus HOIO selectivity of the electrode, we prepared a HOIO sample with less HOI contamination. Moreover the sulfuric acid concentration was increased to 1 M, where the iodic acid disproportionation is slower, and the rate of eq 2, consequently, the corrosion potential due to HOIO could be higher.

In a first series of experiments the response of the electrode was followed after the injection of HOIO, and it was assumed that the potential jump was due dominantly to HOIO and the much smaller HOI content had no significant effect. With that assumption HOIO gave a close to Nernstian potential response, analogous to the one observed with HOI, but the HOIO calibration line was considerably below that of the HOI. Such a behavior could be explained with the corrosion potential theory and could be described by a Nicolsky-type equation³⁷ for the electrode potential where both HOIO and HOI are fast corrosive agents. Nevertheless, an alternative explanation, that the observed close to Nernstian response was still due to the minor HOI contamination of the HOIO sample, could not be excluded either.

Thus, in a second series of experiments, to eliminate safely any interference due to HOI, we applied also resorcinol, which is a very effective HOI scavenger. That way it was possible to prove convincingly that a nonzero corrosion signal caused by HOIO really exists. However, that signal was found to be rather weak and the experiments gave a non-Nernstian calibration

diagram with a slope of about 20 mV/decade, characteristic for slow corrosion processes.³⁵

Due to the non-Nernstian response for HOIO, the HOI versus HOIO selectivity cannot be characterized by a usual Nicolsky-type selectivity coefficient. If we assume, however, that the corrosion of the electrode by HOI and HOIO proceeds independently then a generalized Nicolsky-type (GN) equation can be derived as it is shown in the Supporting Information. To test that formula, we wanted to compare measured and calculated electrode potentials in different HOI–HOIO mixtures.

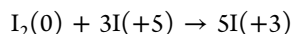
In the course of the disproportionation process of HOIO (eq3), the HOI/HOIO concentration ratio is changing continuously. It starts from a very low value to reach high values later. Thus, the process seemed to be an ideal testing ground for the GN equation. The kinetics of the disproportionation of HOIO was simulated, and the calculated electrode potential versus time curves were compared with the experimental ones. It was found, however, that disregarding the first 50–70 s long transition period (which was due to the response time of the electrode) calculations assuming that the electrode responds to HOI only gave better fittings of the experimental and calculated curves than calculations applying the GN equation. This result suggests that the hypothesis of the GN equation, the independence of the corrosion processes, fails, and HOI is able to prevent the electrode somehow from responding to HOIO, even if the latter is present in much higher concentration than HOI. In other words, when HOI is present, the electrode potential is determined by that component exclusively.

That conclusion was also proven by a direct experiment where HOIO was injected in a relatively high concentration into a 30X more dilute HOI solution without causing any detectable instantaneous change of the electrode potential. As in numerous oxyiodine reaction systems (like in BL or BR oscillators and their subsystems) the concentration ratios are just the opposite (HOI is usually present in much higher concentrations than HOIO), we can conclude that in such systems the electrode potential is governed by HOI selectively and any interference due to HOIO can be neglected.

■ EXPERIMENTAL SECTION

Chemicals. KIO_3 (Sigma-Aldrich, ACS reagent, 99.5%), KI (Riedel-deHaën, puriss. p. a.), resorcinol (Fluka purum >98%), H_2SO_4 (96%, Thomasker, p.a.), AgNO_3 (Reanal, p.a.) and I_2 (Reanal, p.a.) were used as received. All solutions were prepared with double-distilled water.

Preparation of I(+3) solutions “I(+3)-C” and “I(+3)-D” in 96% H_2SO_4 . Production of I(+3) from iodine and iodate in 96% sulfuric acid is based on the following stoichiometry:³⁸



The following recipe is a modification of an earlier one.³⁵ One difference is that a slightly higher I(+5)/ $\text{I}_2(0)$ ratio was applied now, namely 8.3 (and sometimes more) instead of 8, to obtain an I(+3) solution contaminated with less I(+1). More importantly, iodine was applied not in a solid form but it was dissolved in dichloromethane (DCM), which trick accelerated the dissolution of iodine and the production of I(+3) considerably.

Solution I(+3)-C (“C” denotes “concentrated”) was prepared by dissolving first 43 mg ($\sim 200 \mu\text{mol}$) KIO_3 in 2.5 mL of 96% H_2SO_4 in a test tube. Then 6 mg ($\sim 24 \mu\text{mol}$) of I_2 was

dissolved in 1 mL of DCM and the purple iodine solution was layered on the top of the more dense KIO_3 solution. A gentle stirring with a small magnetic stirrer bar was applied until the color of iodine disappeared from the organic phase within 5–10 min. Solution I(+3)-C is the lower sulfuric acid phase, which was separated from the upper organic phase. It was used without further dilution for experiments where higher I(+3) concentrations were needed.

In accordance with the production stoichiometry and assuming a 100% yield, 120 μmol of I(+3) could be expected meaning a theoretical 48 mM I(+3) concentration in solution I(+3)-C. The experimentally found I(+3) concentration in the sulfuric acid phase is less than the theoretical yield, however, as some I(+1) and I(+3) can dissolve in the organic phase as well. (The maximum yield was about 84%. A method to determine I(+3) concentrations is discussed later.)

Solution I(+3)-D (“D” stands for “diluted”) was applied in experiments requiring lower I(+3) levels, and it was obtained from solution I(+3)-C via dilution by a factor of 10 with 96% H_2SO_4 . That factor is two times higher than earlier.³⁵ This way solution I(+3)-D has a long time stability: according to our measurements its I(+3) concentration remained constant at least for half a year when it was stored at -15°C in the refrigerator.

For practical reasons, we always prepared only small amounts of I(+3)-C solutions requiring only a few milligrams of iodine which method caused some weighing errors. Moreover, in some cases, we used even less iodine to suppress I(+1) formation and decrease the I(+3) concentration to avoid a too rapid I(+3) disproportionation when solution I(+3)-C is injected into 1 M H_2SO_4 . Thus, the actual concentration of the I(+3) stock solutions prepared at different times was always determined by titration before the experiments. For example, the I(+3) concentration of the stock solution I(+3)-D applied in experiments shown in Figure 1 was 4.03 mM, indicating a $(4.03/4.8) \times 100 = 84\%$ yield. [The I(+3) concentration of the stock was calculated from a titration result indicating an initial HOIO concentration of 21.9 μM in the reactor after injecting 300 μL of I(+3)-D into a reactor volume of 55.2 mL.]

Solutions of I(+1) in DCM were prepared as previously.³²

Electrodes and the Measuring System. Instead of a commercially available iodide selective electrode, a homemade Ag/AgI indicator electrode was used. It was prepared by covering a high purity silver wire with molten AgI. The details of the preparation are given in our previous publication.³² The Ag/AgCl reference electrode was filled with a solution of 0.1 M KCl in 1 M sulfuric acid. The “salt” bridge also contained 1 M sulfuric acid (but without any KCl) to minimize liquid junction potentials.

The electromotive force of the galvanic cells was measured with a Keithley model 2000 multimeter equipped with a Model-2000-scanner card connected to a computer which collected EMF values every 0.5 s.

For titrations an ISMATEC REGLO DIGITAL peristaltic pump equipped with a 0.19 mm inner diameter tubing was applied.

Determination of the I(+3) Content of I(+3) Solutions by Titration with Iodide. Figure 1 shows various titration experiments applying diluted stock solution I(+3)-D. The experiments were started by filling 50 mL of 1 M sulfuric acid solution into a magnetically stirred reactor thermostated to 25°C and equipped with an AgI indicator and an Ag/AgCl reference electrode. After a 5 min waiting period, a variable

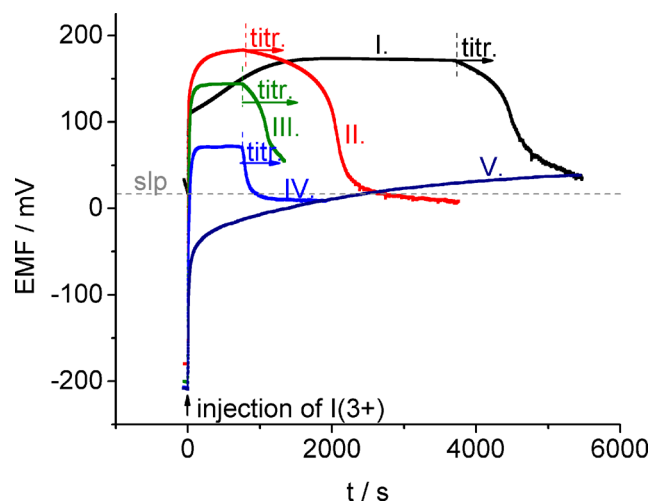


Figure 1. Experiments to develop a HOIO measuring method. The curves display the potential changes of an AgI indicator electrode during titration with a 1 mM iodide solution. $[\text{H}_2\text{SO}_4] = 1\text{ M}$, $T = 25^\circ\text{C}$ in all experiments of this work. At $t = 0$, 300 μL of stock solution I(+3)-D was injected into the reactor containing variable concentrations (I–V) of iodide. The injection was followed by a reaction time t_R before starting the titration. Flow rate of the titrant: 0.77 $\mu\text{L/s}$ 1 mM KI into 55.2 mL reactor volume. [I(+1)] is the HOI concentration in the reactor found by titration. For further technical details see Experimental Section.

amount of 1 mM KI and distilled water was pipetted into the reactor. The sum of the volumes of the KI solution V_I and the distilled water V_W was 5 mL in all experiments. Then the electrode potential recording was started, and 300 μL of I(+3)-D was injected into the reactor to give a total liquid volume of 55.2 mL there. With this technique, sulfuric acid concentration changes due to the addition of the 5 mL aqueous solution and the injection of 300 μL of I(+3)-D (in 96% H_2SO_4) cancel each other out and the H_2SO_4 concentration in the reactor remained $\sim 1\text{ M}$ (increasing less than 1%) after these manipulations. The technique helped to keep liquid junction potential drifts caused by changes in the sulfuric acid concentration at a minimum.

In experiment I, no iodide was present ($V_I = 0\text{ mL}$, $V_W = 5\text{ mL}$). Curve I shows the potential response of an AgI electrode for the increasing HOI concentration generated by the slow disproportionation of the injected HOIO. After 3700 s, the HOI produced this way was titrated with 1 mM KI solution with a 0.77 $\mu\text{L/s}$ flow rate.

In experiments II–V, some initial iodide was present and the product was titrated after 750 s reaction time. In experiments II, $V_I = 1.2\text{ mL}$ ($V_W = 3.8\text{ mL}$); III, $V_I = 3.0\text{ mL}$ ($V_W = 2.0\text{ mL}$); IV, $V_I = 3.6\text{ mL}$ ($V_W = 1.4\text{ mL}$); and V, $V_I = 4.2\text{ mL}$ ($V_W = 0.8\text{ mL}$). In the last experiment, no titration was performed because iodide was already in excess.

Calibration of the AgI Electrode for Ag^+ and I^- . Fifty milliliters of 1 M H_2SO_4 was filled into the reactor where the AgI and the Ag/AgCl electrodes were already present. Then an AgNO_3 or KI solution was added, respectively, in increasing quantities, establishing first a concentration of $\sim 2\text{ }\mu\text{M}$ and then increasing the concentration by a factor of about 2 in each step. First 1 mM solutions were added (100, 100, 200, 400, and 800 μL) and then 10 mM solutions (200, 400, and 800 μL), so the concentrations were 2.0, 4.0, 7.9, 15.7, 31.0, 69.5, 146, and 294 μM for AgNO_3 and KI, respectively.

Calibration of the AgI Electrode for HOI. First, 50 mL of 1 M H_2SO_4 was filled into the reactor where the AgI and the Ag/AgCl electrodes were already present, and then 100 μL of I(+1) solution in DCM was injected into the reactor where continuous stirring was maintained. This moderate initial concentration of HOI was chosen to reduce the loss due to its disproportionation. The solution was then titrated with 0.01 M KI solution and from the result of the titration the initial HOI concentration was calculated. Then, knowing the initial value and the amount of the added KI, HOI concentrations in the course of the titration were calculated. The calibration diagram was created by plotting the measured EMF values against the logarithm of these calculated HOI concentrations.

A small deviation from a straight semilogarithmic calibration line was observed at HOI concentrations below 1 μM . (The measured EMF values deviated downward from the line in that concentration region.) It is possible that the deviation is due to some HOIO contaminating the HOI solution. While HOIO cannot affect the electrode potential in the presence of HOI (as will be shown later), it contributes to the KI consumption during the titration leading to an overestimated HOI concentration. Another possibility is that the deviation is caused by a too long electrode response time, which is increasing with a decreasing HOI concentration.

Calibration of the AgI Electrode for HOIO. First 50 mL of 1 M H_2SO_4 was filled into the reactor where the AgI and the Ag/AgCl electrodes were already present. Then a variable volume V_1 of the I(+3)-D or the I(+3)-C stock solution was injected into a conical flask containing 17 mL of water and a variable volume V_2 of 96% H_2SO_4 . [The I(+3) concentration of the stock solutions applied in these experiments was 2.76 mM for I(+3)-D and 18.6 mM for I(+3)-C, respectively.] The sum $V_1 + V_2$ was always 1.0 mL, thus the final sulfuric acid concentration in the flask was about 1.02 M in all cases. After about 5–10 s of vigorous shaking, the HOIO solution produced this way (with a total volume of about 17.7 mL) was poured into the magnetically stirred reactor. This way the change of the sulfuric acid concentration was less than 0.5%. The aim of the procedure, however, was not only to avoid pH changes in the reactor but also to achieve a more rapid and more reproducible mixing there in the most critical initial phase of the experiment. Most importantly, applying this procedure, the heat of mixing was the same in all experiments.

The above procedure was applied in Figures 3–5. In these experiments aqueous solutions containing I(+3) in the form of HOIO were injected to the reactor, in contrast with the experiments shown in Figure 1, where I(+3) was in a 96% H_2SO_4 medium when injected. That difference is indicated in the Figures by writing “injection of I(+3)” near the arrow in Figure 1 but writing “injection of HOIO” in Figures 3–5. Another difference is that the aqueous solutions contain small but non-negligible amounts of HOI produced from HOIO by disproportionation during the shaking period.

In the first series of experiments, the volume of the added I(+3) stock solution V_1 was 100, 200, 500, and 1000 μL of I(+3)-D and 200 μL of I(+3)-C. The EMF versus time diagrams of these experiments are shown in Figure 2 as curves I–V.

Then, as a preliminary experiment, $V_1 = 500 \mu\text{L}$ of I(+3)-C was used and 17 s after the start of the disproportionation 120 μL 0.01 M resorcinol was injected. The result of that experiment is shown in Figure 4a.

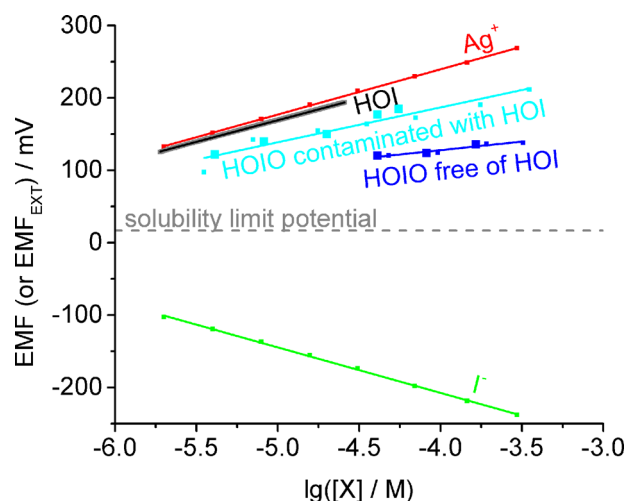


Figure 2. Semilogarithmic calibration lines of the molten-type AgI electrode for Ag^+ and I^- ions (equilibrium EMF values), for HOI (steady state EMF values), and for HOIO (extrapolated EMF_{EXT} values) in 1 M H_2SO_4 . There are two different HOIO lines. The upper one is obtained from experiments like the ones shown in Figure 3 (the five data points obtained from Figure 3 are marked with large squares), while the lower one is obtained from experiments like the ones shown in Figure 4b (the three data points obtained from Figure 4b are marked with large squares) when resorcinol was also present.

Next, in a second series of experiments, 0.01 M resorcinol was also added in variable volumes V_R to the 50 mL of 1 M H_2SO_4 in the reactor before injecting there the 17.7 mL of HOIO solution. The results of these experiments are shown in Figure 4b as curves I–III. Experiment I: $V_R = 50 \mu\text{L}$, $V_1 = 150 \mu\text{L}$ of I(+3)-C; II: $V_R = 100 \mu\text{L}$, $V_1 = 300 \mu\text{L}$ of I(+3)-C; and III: $V_R = 200 \mu\text{L}$, $V_1 = 600 \mu\text{L}$ of I(+3)-C.

RESULTS AND DISCUSSION

The HOI/HOIO selectivity of our molten-type AgI electrode³² was tested by monitoring the disproportionation of HOIO in a

Table 1. Slope s and Intercept EMF_0 Values for Various Calibration Lines Shown in Figure 2

X	s (mV/decade)	EMF_0 (mV) at $[X] = 1 \text{ M}$
I^-	−62.9	−459
Ag^+	62.6	490
HOI	62.1	479
HOIO contaminated with HOI	48.1	379
HOIO free of HOI	23.7	223

1 M sulfuric acid where the ratio $r = [\text{HOI}]/[\text{HOIO}]$ increased monotonically from $r \ll 1$ to $r > 1$ in the course of the reaction. To start the reaction I(+3) stock solutions were injected into the 1 M sulfuric acid medium. (Recipes of stock solutions I(+3)-C and I(+3)-D, prepared with 96% H_2SO_4 as a solvent, are given in Experimental Section.) Besides I(+3), the stock solutions also contain some I(+5) and I(+1) but the latter has a relatively small or negligible concentration. All of these iodine species are in the form of various oxides (or anhydrides) in the 96% H_2SO_4 solvent but, after the injection into the aqueous sulfuric acid medium, I(+5), I(+3), and I(+1) appear as IO_3^- , HOIO, and HOI, respectively, and the disproportionation of HOIO starts promptly.

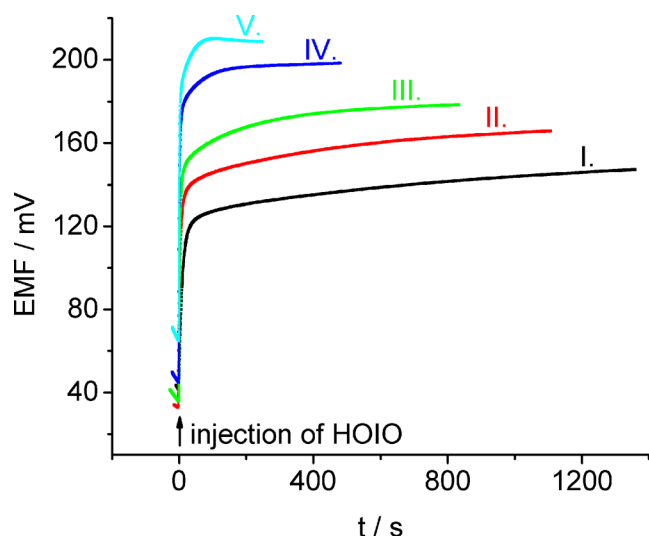
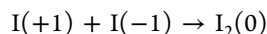
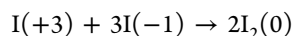


Figure 3. Potential response of the AgI electrode after the injection of iodosous acid into a 1 M H_2SO_4 medium. I. $[\text{HOIO}]_0 = 4.1 \mu\text{M}$; II. $[\text{HOIO}]_0 = 8.2 \mu\text{M}$; III. $[\text{HOIO}]_0 = 20 \mu\text{M}$; IV. $[\text{HOIO}]_0 = 41 \mu\text{M}$; and V. $[\text{HOIO}]_0 = 55 \mu\text{M}$.

In theory, the AgI electrode potential might be affected by all the three iodine species. It is known,³² however, that acidic IO_3^- has no effect even in millimolar concentrations, and the concentration of the presently used solutions is in the micromolar range. It is also known from earlier experiments^{32,34} that AgI electrodes give a Nernstian potential response to HOI in micromolar concentrations and above, but no information was available about the potential response caused by HOIO, especially in the presence of HOI. Thus, the immediate aim of the research was to obtain an experimental calibration curve for HOIO. To this end, as a first step, a reliable method to measure HOIO concentration by titration with iodide was developed.

Determination of I(+3) by Titration with Iodide.

Titration of HOIO and HOI is based on their reactions with I^- in a 1 M sulfuric acidic medium with the following redox stoichiometries:



$\text{I}(+3)$ solutions I(+3)-C or I(+3)-D were injected into 1 M sulfuric acid medium where iodide was also present in variable concentrations. Figure 1 shows EMF versus time curves recorded in such experiments applying a molten-type AgI indicator electrode.

$$[\text{I}^-]_0 = 0, t_R = 3700 \text{ s}, [\text{I}(+1)] = 11.1 \mu\text{M} \quad (\text{I})$$

$$[\text{I}^-]_0 = 21.7 \mu\text{M}, t_R = 750 \text{ s}, [\text{I}(+1)] = 18.6 \mu\text{M} \quad (\text{II})$$

$$[\text{I}^-]_0 = 54.3 \mu\text{M}, t_R = 750 \text{ s}, [\text{I}(+1)] = 5.1 \mu\text{M} \quad (\text{III})$$

$$[\text{I}^-]_0 = 65.2 \mu\text{M}, t_R = 750 \text{ s}, [\text{I}(+1)] = 0.6 \mu\text{M} \quad (\text{IV})$$

$$[\text{I}^-]_0 = 76.1 \mu\text{M}, \text{ here no } \text{I}(+1) \text{ remained for titration} \quad (\text{V})$$

To titrate $\text{I}(+3)$, there are two possible strategies. One possibility is to apply no iodide at the beginning but wait until a

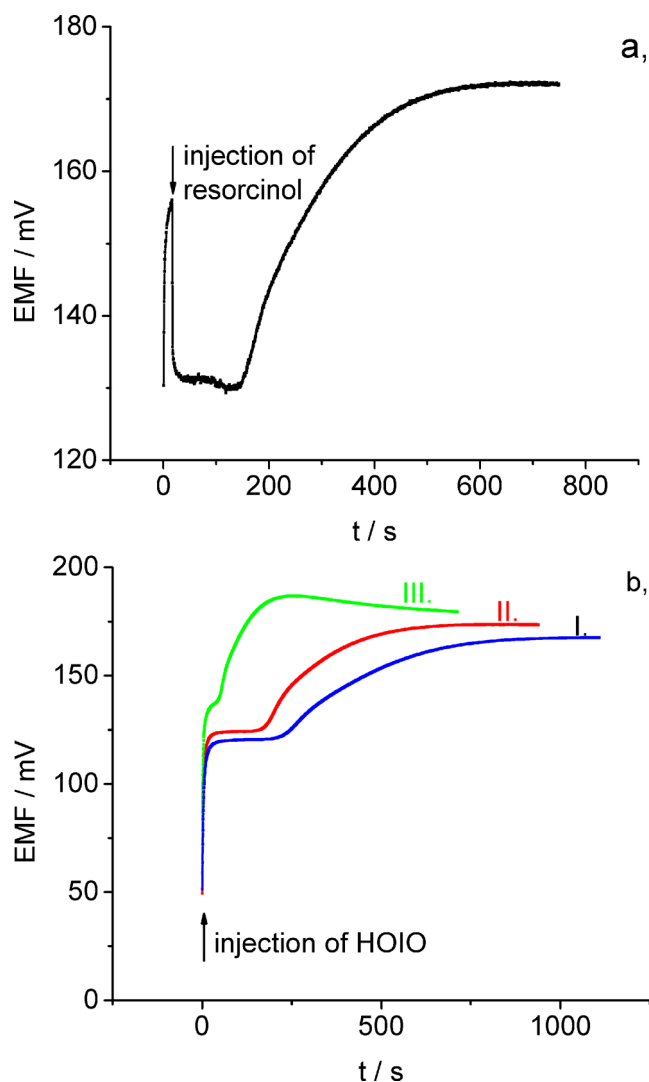
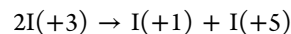


Figure 4. Potential response of the AgI electrode for HOIO in the presence of resorcinol. (a) Injecting resorcinol into a disproportionating HOIO solution. At $t = 0$, an $\text{I}(+3)$ stock was injected into the reactor establishing an initial iodosous acid concentration there $[\text{HOIO}]_0 = 137 \mu\text{M}$. Next, at $t = 17 \text{ s}$, 120 μL of 0.01 M resorcinol was injected, creating at that moment a 18 μM resorcinol concentration in the reactor. (b) Disproportionation of HOIO when resorcinol (res) is present already from the start: I. $[\text{HOIO}]_0 = 41 \mu\text{M}$, $[\text{res}]_0 = 7.4 \mu\text{M}$; II. $[\text{HOIO}]_0 = 82 \mu\text{M}$, $[\text{res}]_0 = 15 \mu\text{M}$; and III. $[\text{HOIO}]_0 = 165 \mu\text{M}$, $[\text{res}]_0 = 30 \mu\text{M}$.

nearly complete disproportionation of HOIO occurs after the injection, with the following stoichiometry:



and in the next step to titrate the produced $\text{I}(+1)$ with iodide. (Such a titration is possible as it was shown earlier.^{32,35}) If we assume that the disproportionation of HOIO is practically complete, moreover we neglect the disproportionation of HOI, then the concentration of the $\text{I}(+3)$ solution $[\text{I}(+3)]_0$ can be calculated as

$$[\text{I}(+3)]_0 = 2[\text{I}(+1)]_\infty$$

where $[\text{I}(+1)]_\infty$ is the measured HOI concentration after a long disproportionation time. (In the above balance equation $[\text{I}(+1)]_0$ was neglected as its concentration is much less than

Table 2. Kinetic Model and the Rate Constants Applied in the Simulations^a

N°	reactions	rate laws	rate constants
R1	$2\text{HOIO} \rightarrow \text{IO}_3^- + \text{IOH} + \text{H}^+$	$r_1 = k_1[\text{HOIO}]^2$	$k_1 = 0.05$
R2	$\text{IOH} + \text{HOIO} \rightarrow \text{IO}_3^- + \text{I}^- + 2\text{H}^+$	$r_2 = k_2[\text{IOH}][\text{HOIO}]$	$k_2 = 160$
R3	$\text{HOIO} + \text{I}^- + \text{H}^+ \rightleftharpoons 2\text{IOH}$	$r_3 = k_3[\text{HOIO}][\text{I}^-][\text{H}^+] - k_{-3}[\text{IOH}]^2$	$k_3 = 4 \times 10^9$; $k_{-3} = 2$
R4	$\text{IOH} + \text{I}^- + \text{H}^+ \rightleftharpoons \text{I}_2 + \text{H}_2\text{O}$	$r_4 = k_4[\text{IOH}][\text{I}^-] - k_{-4}[\text{I}_2]/[\text{H}^+]$	$k_4 = 1.8 \times 10^9$; $k_{-4} = 0.0017$

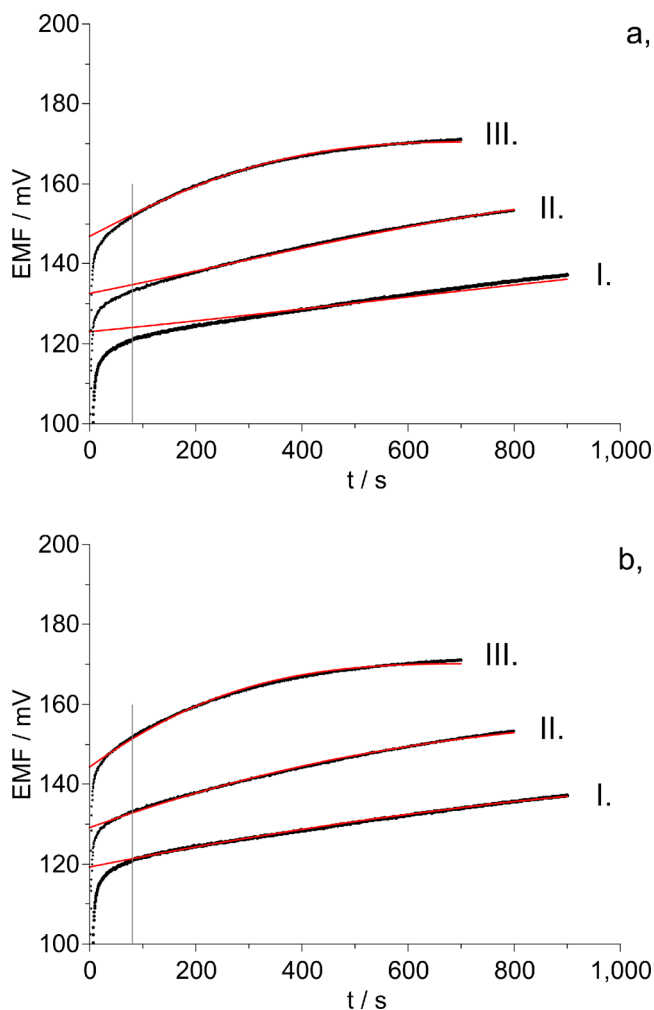
^aConcentration unit, M, and time unit, s.

Figure 5. Measured (black) and simulated (red) electrode potential versus time diagrams in the course of the HOIO disproportionation with three different initial HOIO concentrations. I. $[\text{HOIO}]_0 = 7.42 \mu\text{M}$; II. $[\text{HOIO}]_0 = 12.86 \mu\text{M}$; and III. $[\text{HOIO}]_0 = 25.72 \mu\text{M}$. Data points in the first 80 s were not used for parameter fitting as these values might be affected by the response time of the electrode. (a) Simulation with a generalized Nicolsky-type equation. (b) Simulation with a simple Nernst type equation.

$[\text{I}(+3)]_0$) Experiment I applied that strategy. After 3700 s, the HOI concentration found by titration was $11.1 \mu\text{M}$, thus we can estimate the initial HOIO concentration as $22.2 \mu\text{M}$.

Another method would be to titrate HOIO (and also the HOI formed in this reaction) with iodide so rapidly that disproportionation of HOIO and HOI would be insignificant during the time of titration. That can be achieved if there is enough iodide in the reactor at the time of addition of the HOIO solution as the relatively slow disproportionation reactions are not able to compete with the much faster

Table 3. $\text{EMF}_{0,\text{HOI}}$ and Initial Hypoiodous and Iodous Acid Concentrations Obtained from the Optimum Fit of Simulated and Measured EMF versus Time Diagrams^a

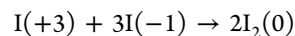
$[\text{HOIO}]_v (\mu\text{M})$	$\text{EMF}_{0,\text{HOI}} (\text{mV})$	$[\text{HOI}]_0 (\mu\text{M})$	$[\text{HOIO}]_0 (\mu\text{M})$
10.0	485.0	1.29	7.42
16.6	484.8	1.87	12.86
33.2	481.3	3.74	25.72

^a $[\text{HOIO}]_v$ (virtual): initial iodous acid concentration disregarding the disproportionation during its preparation by mixing $\text{I}(+3)$ solutions with water (see Experimental Section). $[\text{HOIO}]_0 = [\text{HOIO}]_v - 2[\text{HOI}]_0$.

Table 4. Time τ Above Which the Deviation between the Measured and the Simulated EMF is Less Than 1 mV and the Hypoiodous and Iodous Acid Concentrations at This Moment

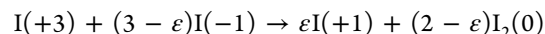
experiment	$\tau (\text{s})$	$[\text{HOI}]_\tau (\mu\text{M})$	$[\text{HOIO}]_\tau (\mu\text{M})$
I	53.5	1.36	7.26
II	28.0	1.97	12.6
III	22.5	4.04	25.0

$\text{I}(+3) - \text{I}(-1)$ and $\text{I}(+1) - \text{I}(-1)$ reactions. In this ideal case, the stoichiometric equation in the equivalence point would be



Then the amount of HOIO can be calculated as one-third of the consumed iodide. To detect the equivalence point in an extremely rapid titration, however, would be problematic. Thus, we applied a two step titration procedure where a large part of the titrant iodide was already present in the reactor when $\text{I}(+3)$ was injected and only the relatively small amount of HOI, remaining after the rapid $\text{I}(+3) - \text{I}(-1)$ and $\text{I}(+1) - \text{I}(-1)$ reactions, was titrated but with a normal rate. The smaller the amount of the remaining HOI the better the result. This is because the rate of the HOI decomposition is proportional to the square of the HOI concentration.

Following these ideas in experiments II–V, some iodide was mixed into the 1 M H_2SO_4 before the injection of $\text{I}(+3)$. (In the following it will be assumed that the $\text{I}(+3)$ solutions do not contain $\text{I}(+1)$ species which is a good approximation for the experiments shown in Figure 1, as we will show later.) In experiments II–IV, the applied iodide was substoichiometric, thus the reaction equation can be written in the following form:



which is a good approximation of the real stoichiometry only when $\varepsilon \ll 1$. Otherwise, not all HOIO will be consumed in the initial $\text{HOIO} - \text{I}^-$ reaction and/or the amount of HOI formed will be higher. Then the disproportionation of HOIO and HOI cannot be neglected during the titration. If ε is small, however, then the initial $\text{I}(+3)$ concentration can be calculated as

$$[\text{I}(+3)]_0 = ([\text{I}(-1)]_0 + [\text{I}(+1)]_R) / 3$$

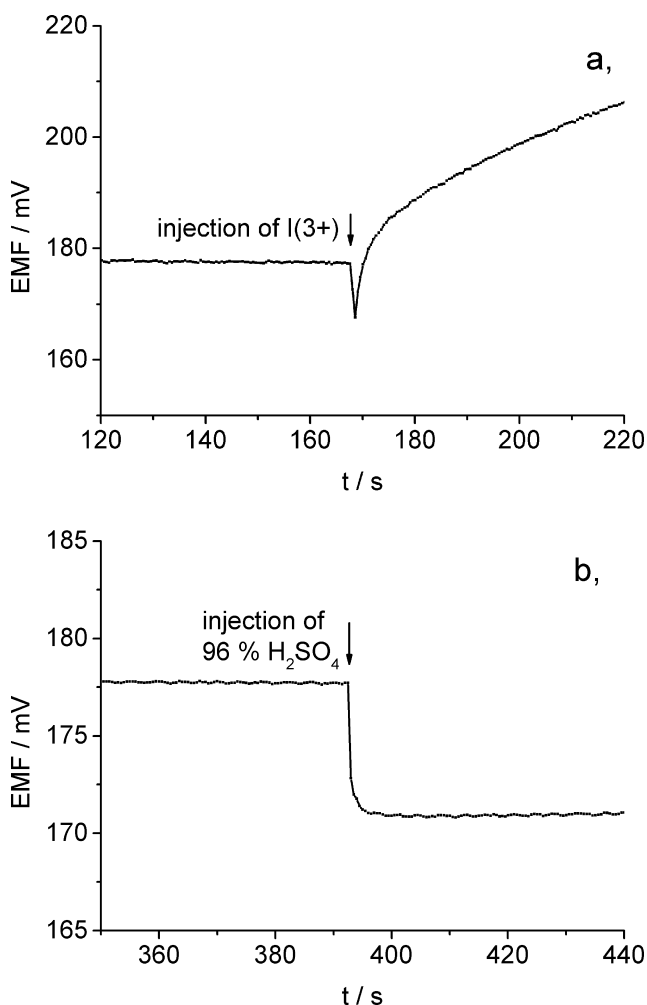


Figure 6. Potential response of a molten-type AgI electrode. (a) At $t \approx 168$ s, $320 \mu\text{L}$ of $\text{I}(+3)\text{-C}$ solution (in $96\% \text{H}_2\text{SO}_4$) was injected into the reactor, which already contained 50 mL of $12.5 \mu\text{M}$ HOI solution (in $1 \text{ M H}_2\text{SO}_4$). HOIO concentration right after the injection: $356.4 \mu\text{M}$. (b) Injection of $320 \mu\text{L}$ of $96\% \text{H}_2\text{SO}_4$ [without any $\text{I}(+3)$] into 50 mL of $12.5 \mu\text{M}$ HOI solution caused practically the same potential drop.

where $[\text{I}(-1)]_0$ is the initial iodide concentration in the reactor and $[\text{I}(+1)]_R$ is the $\text{I}(+1)$ concentration determined by titration after the reaction of $\text{I}(+3)$ and $\text{I}(-1)$. As experiment IV should have the smallest positive ε value, it is reasonable to calculate $[\text{HOIO}]_0$ from that experiment:

$$[\text{HOIO}]_0 = \frac{65.2 \mu\text{M} + 0.6 \mu\text{M}}{3} = 21.9 \mu\text{M}$$

The result obtained with this second method is more reliable as the assumptions applied to calculate it are more realistic.

While the $[\text{HOIO}]_0$ concentrations obtained by the first and the second method are rather close (22.2 vs $21.9 \mu\text{M}$), most probably this is only incidental because the errors involved in experiment I (an incomplete disproportionation of HOIO and some decomposition of HOI) have opposite effects. Moreover, the second method requires less time. Thus for HOIO concentration determination, we always applied the method as shown in experiment IV: we applied first an iodide amount which was enough to eliminate all HOIO and nearly all of the HOI produced in the HOIO-I^- reaction, and only the

remaining low level of HOI was titrated. This method required some rough preliminary titrations, however.

To add too much iodide (negative ε) should be also avoided because then no $\text{I}(+1)$ remains for titration. In that case, the excess iodide reacts slowly with the iodate content of the reaction mixture as experiment V shows.

Finally a remark. In the above stoichiometric calculations, it was assumed that the $\text{I}(+1)$ content of the $\text{I}(+3)$ stock solutions is relatively small and can be neglected in the calculations. But small is obviously not zero, thus it would be useful to measure or estimate its level somehow. Regarding the initial potential jump of experiment I and using the calibration line for HOIO free of HOI in Figure 2 that jump could be explained, however, by the injected $\text{I}(+3)$ alone, and any correction due to some initial HOI would be within the experimental error. In the absence of a measured value we applied equation S11 of the Supporting Information to estimate an upper limit for the initial HOI concentration. In accordance with that equation, a $0.6 \mu\text{M}$ HOI contamination in a $22 \mu\text{M}$ HOIO solution would cause a 10 mV potential increase that would be easy to detect. On the basis of that result, we can say that the $\text{I}(+1)$ contamination of the $\text{I}(+3)$ stock is certainly less than 3% .

Calibration of the AgI Electrode for Ag^+ , I^- , and HOI.

Calibration methods for Ag^+ and I^- ions and for the corrosive agent HOI are described in Experimental Section. Calibration lines obtained with these methods are shown in Figure 2.

The slope and the intercept values of the calibration lines are given in Table 1.

The slope values were reproducible within $\pm 1 \text{ mV}$, but the intercept values could change $\pm 5 \text{ mV}$ from 1 day to another due to some unidentified memory effects of the electrode. To obtain a somewhat better day-to-day reproducibility would have been possible but only by keeping the electrode in an appropriate annealing solution for several hours before each series of measurement. Such lengthy procedures, however, were not necessary here as the EMF_0 value changed less than 1 mV within one series of measurement and its optimal value for that series could be determined by curve fitting.

Similar calibration lines for Ag^+ , I^- , and HOI have been already measured previously³² but in $25 \text{ mM H}_2\text{SO}_4$. Here the sulfuric acid concentration was increased to 1 M in the hope that HOIO would be more corrosive and would produce a higher corrosion potential in this more acidic medium. The change in the sulfuric acid concentration, however, had some effect on the slope and the intercept of all calibration lines especially below $30 \mu\text{M}$. As Table 1 indicates in $1 \text{ M H}_2\text{SO}_4$, the measured slopes of the Ag^+ , I^- , and HOI lines are about 3 mV/decade higher than the theoretical 59 mV/decade , while in $25 \text{ mM H}_2\text{SO}_4$ they were 2 mV/decade lower than that. The most important change, however, was a downward shift in the position of the Ag^+ calibration line: for example in a $10 \mu\text{M Ag}^+$ ion solution, the measured EMF value was $35 \pm 5 \text{ mV}$ lower than it was in $25 \text{ mM H}_2\text{SO}_4$. The I^- calibration line was also shifted down but by $9 \pm 5 \text{ mV}$ only. As a consequence of these changes, the solubility limit potential decreased to 18 mV (from 36 mV), while the calculated solubility product increased from 7.45×10^{-17} to $7.59 \times 10^{-16} \text{ M}^2$. (We believe, however, that this calculation overestimates the solubility product. This is because while the steep, 62 mV/decade , calibration lines in the low concentration region are real but the measured potentials in this range do not reflect true thermodynamic equilibria, otherwise the slopes would be 59 mV/decade . Consequently,

an equilibrium property like solubility product cannot be estimated safely from such data.)

The downward shift in the position of the Ag^+ calibration line can be attributed most probably to a combined effect of the decreased ionic activity coefficient γ in 1 M H_2SO_4 and maybe to some complex formation between Ag^+ and sulfate ions.³⁹

The reason for the small downward shift in the position of the I^- calibration line is not clear. As the electrolyte in the reference electrode is also 1 M H_2SO_4 , one would expect similar changes in the activity coefficient of the I^- and Cl^- ions, consequently, no shift in the position of the I^- line. The shift is in the order of the estimated experimental error, however.

Another interesting consequence of the downward shift in the position of the Ag^+ line is that the Ag^+ and HOI calibration lines get much closer to each other in a 1 M H_2SO_4 . The distance between the two lines here is a mere 9 ± 5 mV at a $[\text{X}] = 10 \mu\text{M}$ concentration, while that was 37 ± 5 mV in 25 mM H_2SO_4 . The distance predicted by the corrosion potential theory [applying formula (8) in ref 32] is somewhat larger: it is 12 ± 5 mV but still well within the experimental error. We remark here that the increased ionic strength can probably decrease the activity coefficient of silver ions more than that of HOI as the nonprotonated fraction of HOI is not an ionic species.

Calibration of the AgI Electrode for HOIO. Known $[\text{HOIO}]_0$ concentrations were created in the reactor by injecting different amounts of the I(+3) stocks, or their diluted solutions, whose I(+3) content was determined with the titration method described previously. Our aim was to obtain an approximate calibration diagram by plotting the “initial EMF” values against the logarithm of the $[\text{HOIO}]_0$ values. That idea was based on the following five assumptions: (i) during the first minute after the injection, the relative change of the iodous acid concentration is small, thus within this period

$$[\text{HOIO}] \approx [\text{HOIO}]_0$$

as the disproportionation rate of HOIO is relatively slow in 1 M sulfuric acid; (ii) the response time of the electrode is short enough (i.e., it does not influence the measured EMF versus time diagram significantly), disregarding the period of rapid concentration changes in the first 30 s after the injection; (iii) an approximate EMF_{EXT} value can be obtained by linear extrapolation back to $t = 0$ using EMF values measured in the time interval $30 \text{ s} < t < 60 \text{ s}$; (iv) $[\text{I}(+1)]$ contaminating the I(+3) stock solutions is relatively small, consequently $[\text{HOIO}]_0$ is several times larger than $[\text{HOI}]_0$; and (v) in a mixture where HOIO is a major and HOI is only a minor component, the corrosion of the electrode and, consequently, the corrosion potential should be dominated, or at least affected in a certain extent, by $[\text{HOIO}]$.

The experimental EMF versus time diagrams are given in Figure 3.

The calibration diagram [EMF_{EXT} values plotted against $\log([\text{HOIO}]_0)$ calculated from the data of Figure 3] is shown in Figure 2, and it is marked as “HOIO contaminated with HOI”. That name itself indicates that this calibration line is probably artifact. Two serious doubts emerge:

First, if HOIO were a fast corrosive agent as HOI then the diagram would be a straight line but with a slope of 59 mV/decade, at least approximately. The measured slope, however, is only 48.1 mV/decade (see Table 1). (The intercept of the calibration line is also smaller for HOIO than for HOI, but that

could be understood if we assumed that HOIO was a fast but somewhat slower corrosive agent than HOI.)

Second, the measured points on the diagram are rather scattered indicating irreproducibility. As the I(+3) content of the stocks is well-defined, the error is probably due to a minor component, like I(+1) for example, whose concentration is less reproducible in the experiments. At this point, we started to suspect that the fifth assumption of our theory, that EMF_{EXT} values are determined by $[\text{HOIO}]_0$ mostly, might fail, and even a relatively low level $[\text{HOI}]_0$ can have a strong influence on the EMF_{EXT} values. In that case, the poor reproducibility and the close to 59 mV/decade slope might be explained by the presence of some HOI contamination in the HOIO solutions. That HOI can be formed from HOIO during the somewhat less reproducible “shaking period” (see the Calibration of the AgI Electrode for HOIO in Experimental Section).

To test the I(+1) contamination hypothesis, we injected a small amount of resorcinol into a fresh HOIO solution right after the start of its disproportionation as it is shown in Figure 4a. Resorcinol reacts with HOI extremely rapidly, but it also reacts rather fast with HOIO as independent spectrophotometric experiments prove (not shown here).

What can be seen in Figure 4a is compatible with the hypothesis that some contaminating HOI is present already at the start. After the injection of resorcinol, the potential drops sharply by more than 20 mV, which can be interpreted so that resorcinol eliminated the corrosive HOI from the mixture. The remaining 130 mV is still a corrosion potential, however, as it is definitely above the SLP and that should be attributed entirely to HOIO as after eliminating HOI, no other corrosive agent remains in the solution. In the following 100 s, the potential stays around 130 mV and then it starts to rise again. The rise of the potential indicates that the supply of all HOI scavenging organic compounds (including resorcinol and its iodinated and/or oxidized products) is exhausted, leaving room for the unperturbed autocatalytic growth of HOI.

From the preliminary experiments of Figure 4a, we concluded that real HOIO calibration curves can be measured only if all contaminating HOI is eliminated from the solution. Thus, we repeated our experiments in the presence of some resorcinol which was added to the reactor before the injection of I(+3). The potentiometric traces of such experiments are shown in Figure 4b. The $[\text{HOIO}]_0/[\text{res}]_0$ ratio was about 5.6 in all experiments. The excess of HOIO over resorcinol is important because not only HOI but also HOIO can react with resorcinol. With regard to only the close to linear regions appearing on all curves after the injection, the EMF_{EXT} values can be obtained by extrapolation to the time of the injection. The HOIO calibration line obtained this way is shown in Figure 2 (marked as “HOIO free of HOI”).

Simulation of Potentiometric Traces Recorded in HOIO Disproportionation Experiments. As can be seen from the calibration diagrams (Figure 2), an EMF value above the solubility limit potential is due either to Ag^+ ions, or to HOI, or to HOIO. Beside the pure components, we rather often deal with the mixture of the two corrosive components. The calibration diagrams in Figure 2, however, can be used only in the case of pure HOI or HOIO solutions. But what if we have a mixture of the two? This is a relevant problem when dealing with the BL and BR oscillators, for example, and also in the more simple reaction of the HOIO disproportionation.

As it is shown in the Supporting Information, the EMF of a HOI–HOIO mixture can be calculated from the concentration

of the corrosive agents and from their individual calibration lines with the help of a generalized Nicolsky-type (GN) equation. The GN equation is based on the hypothesis that the corrosion of the AgI electrode by HOI and by HOIO are independent processes.

As the autocatalytic kinetics of the HOIO disproportionation is rather well-known,^{35,40} we decided to use it to test the validity of the GN equation. The kinetic model applied here and given in Table 2 is based on a recent paper by two of the authors of this paper (G.S. and S.D.F.).⁴¹

First, the EMF versus time diagrams were calculated from the simulated HOI and HOIO concentration versus time diagrams, applying the generalized Nicolsky-type (GN) equation as that is given by eq S11 of the Supporting Information. Initial $[I(+3)]$ was determined by titration. For each curve, two parameters, $EMF_{0,HOI}$ and $[HOI]_0$, were varied to obtain an optimum fit of the calculated curves to the measured ones. The result is shown in Figure 5a.

Next, we wanted to check whether the GN equation really gives a better result than a more simple expression where we neglect the correction term containing the HOIO concentration. In that case, eq S11 of the Supporting Information goes back to the calibration diagram for HOI:

$$EMF \text{ (mV)} = EMF_{0,HOI} + 62.1 \log([HOI]_B)$$

which is a Nernstian type equation. Here $[HOI]_B$ is the HOI concentration in the bulk. The result of curve fitting with this equation can be seen in Figure 5b. An unexpected result was obtained: the simple Nernst equation produced a better fit than the more complex GN equation. Table 3 shows the fixed and fitted parameters for Figure 5b. Table 4 shows hypiodous acid and iodous acid concentration at a time τ when the difference between the simulated and the calculated EMF curves drops below 1 mV (also for Figure 5b). It is interesting to observe that at this point the iodous acid concentration is still 5–7 times higher than that of the hypiodous acid. In spite of that the measured EMF value is not affected by the much larger HOIO concentration, even the small correction predicted by the GN equation cannot be detected experimentally.

Direct Test to Prove the High HOI/HOIO Selectivity of the Electrode. In the previous paragraph, the main conclusion was that HOIO cannot affect the electrode potential even in cases where the GN equation would predict such an effect. Figure 6 presents a more direct experimental evidence to support that conclusion. First a rather low (12.5 μM) HOI concentration was established in the reactor, then, after a steady electrode potential was achieved, an $I(+3)$ solution was injected to increase the HOIO concentration in a nearly stepwise manner to 356.4 μM , which is nearly 30 times higher than that of HOI. The potential response is shown in Figure 6a. Right after the injection, as can be seen, not an immediate potential jump but a sharp potential drop appeared. That drop is due to a change of the liquid junction potential caused by the increased sulfuric acid concentration [remember that $I(+3)$ is in 96% H_2SO_4 , while HOI is in 1 M H_2SO_4]. A separate experiment shown in Figure 6b with the same amount of sulfuric acid but without $I(+3)$ gave practically the same potential drop.

A gradual increase of the potential following its drop shown in Figure 6a is due to the appearance of additional HOI coming from the HOIO disproportionation as in other experiments. If the added HOIO could increase the corrosion potential by 7.5 mV as the GN equation predicts, then practically no decrease or even a small increase would appear in the electrode

potential. However, we were not able to observe such an effect within the experimental error.

The failure of the GN equation can be rationalized if we assume that HOI is able to react with solid AgI, while the $\text{HOIO}-\text{I}^-$ reaction can proceed only in the liquid phase. If this is the case then Ag^+ ions generated by the heterogeneous $\text{AgI}-\text{HOI}$ reaction decrease the I^- concentration in the homogeneous liquid phase to such a low level that the rate of the $\text{HOIO}-\text{I}^-$ reaction becomes insignificant compared to the $\text{AgI}-\text{HOI}$ reaction. In other words, the precondition for the validity of the GN equation is not satisfied as the two corrosion reactions are not independent.

Naturally, at high enough HOIO and low enough HOI concentrations, the assumption of independent corrosion processes might be a valid approximation. But in typical aqueous oxyiodine reaction systems like the BL and BR oscillators and their subsystems, usually the HOI concentrations are much higher than that of the HOIO, and in such cases even the GN equation predicts that the electrode is practically insensitive to HOIO changes.

CONCLUSION

The above experiments and calculations support unanimously that, in the presence of HOI, an AgI electrode is practically insensitive to HOIO. In other words, such an electrode has a very high HOI/HOIO selectivity in 1 M sulfuric acid, and its potential will not be affected by HOIO in most cases. The same conclusion holds for the 0.05–0.2 M sulfuric acid media of the BL and BR reactions because the corrosion signal due to HOIO should be even weaker at these lower acidities.

ASSOCIATED CONTENT

Supporting Information

Derivation of a generalized Nicolsky-type equation to estimate the corrosion potential of an AgI electrode in HOI–HOIO mixtures. This material is available free of charge via the Internet at <http://pubs.acs.org>.

AUTHOR INFORMATION

Corresponding Author

*E-mail: wittmann@eik.bme.hu.

Notes

The authors declare no competing financial interest.

ACKNOWLEDGMENTS

This work was partially supported by OTKA Grant K77908.

REFERENCES

- (1) Pillar, E. A.; Guzman, M. I.; Rodriguez, J. M. Conversion of Iodide to Hypiodous Acid and Iodine in Aqueous Microdroplets Exposed to Ozone. *Environ. Sci. Technol.* **2013**, *47*, 10971–10979.
- (2) Carpenter, L. J.; MacDonald, S. M.; Shaw, M. D.; Kumar, R.; Saunders, R. W.; Parthipan, R.; Wilson, J.; Plane, J. M. C. Atmospheric Iodine Levels Influenced by Sea Surface Emissions of Inorganic Iodine. *Nat. Geosci.* **2013**, *6*, 108–111.
- (3) Pechtl, S.; Schmitz, G.; Von Glasow, R. Modelling Iodide–Iodate Speciation in Atmospheric Aerosol: Contributions of Inorganic and Organic Iodine Chemistry. *Atmos. Chem. Phys.* **2007**, *7*, 1381–1393.
- (4) Harrell, J. R.; Lutz, J. B.; Kelly, J. L. On the Volatility and Disproportionation of Hypiodous Acid. *J. Radioanal. Nucl. Chem.* **1988**, *127*, 13–20.
- (5) Bray, W. C. A Periodic Reaction in Homogeneous Solution and its Relation to Catalysis. *J. Am. Chem. Soc.* **1921**, *43*, 1262–1267.

- (6) Bray, W. C.; Liebhafsky, H. A. An Oxide of Iodine, I_2O_2 . An Intermediate Compound. *J. Am. Chem. Soc.* **1931**, *53*, 38–44.
- (7) Matsuzaki, I.; Woodson, J.; Liebhafsky, H. A. pH and Temperature Pulses during the Periodic Decomposition of Hydrogen Peroxide. *Bull. Chem. Soc. Jpn.* **1970**, *43*, 3317–3317.
- (8) Liebhafsky, H. A.; Wu, L. S. Reactions Involving Hydrogen Peroxide, Iodine, and Iodate Ion. V. Introduction to the Oscillatory Decomposition of Hydrogen Peroxide. *J. Am. Chem. Soc.* **1974**, *96*, 7180–7187.
- (9) Kolar-Anić, Lj.; Čupić, Ž.; Anić, S.; Schmitz, G. Pseudo-Steady States in the Model of the Bray–Liebhafsky Oscillatory Reaction. *J. Chem. Soc., Faraday Trans.* **1997**, *93*, 2147–2152.
- (10) Vukojević, V.; Anić, S.; Kolar-Anić, Lj. Investigation of Dynamic Behavior of the Bray–Liebhafsky Reaction in the CSTR. Determination of Bifurcation Points. *J. Phys. Chem. A* **2000**, *104*, 10731–10739.
- (11) Schmitz, G.; Kolar-Anić, Lj.; Anić, S.; Grozdic, T.; Vukojević, V. Complex and Chaotic Oscillations in a Model for the Catalytic Hydrogen Peroxide Decomposition under Open Reactor Conditions. *J. Phys. Chem. A* **2006**, *110*, 10361–10368.
- (12) Ivanović, A.; Čupić, Ž.; Janković, M.; Kolar-Anić, Lj.; Anić, S. The Chaotic Sequences in the Bray–Liebhafsky Reaction in an Open Reactor. *Phys. Chem. Chem. Phys.* **2008**, *10*, 5848–5858.
- (13) Schmitz, G. *Phys. Chem. Chem. Phys.* **2010**, *12*, 6605–6615.
- (14) Schmitz, G. *Phys. Chem. Chem. Phys.* **2011**, *13*, 7102–7111.
- (15) Briggs, T. S.; Rauscher, W. C. Oscillating Iodine Clock. *J. Chem. Educ.* **1973**, *50*, 496–496.
- (16) Furrow, S. D.; Noyes, R. M. The Oscillatory Briggs–Rauscher Reaction. 1. Examination of Subsystems. *J. Am. Chem. Soc.* **1982**, *104*, 38–42.
- (17) *Oscillations and Traveling Waves in Chemical Systems*; Field, R. J., Burger, M., Eds.; Wiley: New York, 1985.
- (18) Epstein, I. R.; Pojman, J. A. *An Introduction to Nonlinear Chemical Dynamics*; Oxford University Press: New York, 1998.
- (19) DeKepper, P.; Epstein, I. R. A Mechanistic Study of Oscillations and Bistability in the Briggs–Rauscher Reaction. *J. Am. Chem. Soc.* **1982**, *104*, 49–55.
- (20) Turányi, T. Rate Sensitivity Analysis of a Model of the Briggs–Rauscher Reaction. *React. Kinet. Catal. Lett.* **1991**, *45*, 235–241.
- (21) Vukojevic, V.; Sorensen, P. G.; Hynne, F. J. Predictive Value of a Model of the Briggs–Rauscher Reaction Fitted to Quenching Experiments. *J. Phys. Chem.* **1996**, *100*, 17175–17185.
- (22) Furrow, S. D.; Cervellati, R.; Amadori, G. New Substrates for the Oscillating Briggs–Rauscher Reaction. *J. Phys. Chem. A* **2002**, *106*, 5841–5850.
- (23) Cervellati, R.; Höner, K.; Furrow, S. D.; Mazzanti, F.; Costa, S. An Experimental and Mechanistic Investigation of the Complexities Arising During Inhibition of the Briggs–Rauscher Reaction by Antioxidants. *Helv. Chim. Acta* **2004**, *87*, 133–155.
- (24) Szabó, G.; Csavdári, A.; Onel, L.; Bourceanu, G.; Noszticzius, Z.; Wittmann, M. Periodic CO and CO₂ Evolution in the Oscillatory Briggs–Rauscher Reaction. *J. Phys. Chem. A* **2007**, *111*, 610–612.
- (25) Onel, L.; Bourceanu, G.; Wittmann, M.; Noszticzius, Z.; Szabó, G. I(+1) Transfer from Diiodomalonic Acid to Malonic Acid and a Complete Inhibition of the CO and CO₂ Evolution in the Briggs–Rauscher Reaction by Resorcinol. *J. Phys. Chem. A* **2008**, *112*, 11649–11655.
- (26) Lawson, T.; Fülöp, J.; Wittmann, M.; Noszticzius, Z.; Muntean, N.; Szabó, G.; Onel, L. Iodomalonic Acid as an Anti-Inhibitor in the Resorcinol Inhibited Briggs–Rauscher Reaction. *J. Phys. Chem. A* **2009**, *113*, 14095–14098.
- (27) Furrow, S. D.; Aurentz, D. J. Reactions of Iodomalonic Acid, Diiodomalonic Acid, and Other Organics in the Briggs–Rauscher Oscillating System. *J. Phys. Chem. A* **2010**, *114*, 2526–2533.
- (28) Cervellati, R.; Greco, E.; Furrow, S. D. Experimental and Mechanistic Investigation of an Iodomalonic Acid-Based Briggs–Rauscher Oscillator and its Perturbations by Resorcinol. *J. Phys. Chem. A* **2010**, *114*, 12888–12892.
- (29) Szabó, E.; Sevcik, P. A Simple Method of Gas Evolution Measurement Suitable for Analysis of Batch Oscillating Reactions: Briggs–Rauscher System with Acetone Revisited. *J. Phys. Chem. A* **2009**, *113*, 3127–3132.
- (30) Szabó, E.; Sevcik, P. Modeling of Interactions Between Iodine Interphase Transport and Oxygen Production in the Modified Briggs–Rauscher Reaction with Acetone. *J. Phys. Chem. A* **2010**, *114*, 7898–7902.
- (31) Onel, L.; Buurmaa, N. J.; Noszticzius, Z. Iodination of Resorcinol by Iodomalonic Acid and Resorcinol Inhibition of the Briggs–Rauscher Oscillatory Reaction, poster presentation at Eu-CheMS Congress, Nuremberg, Germany, Aug 29–Sept 2, 2010.
- (32) Muntean, N.; Lawson, B. T.; Kály-Kullai, K.; Wittmann, M.; Noszticzius, Z.; Onel, L.; Furrow, S. D. Measurement of Hypoiodous Acid Concentration by a Novel Type Iodide Selective Electrode and a New Method To Prepare HOI. Monitoring HOI Levels in the Briggs–Rauscher Oscillatory Reaction. *J. Phys. Chem. A* **2012**, *116*, 6630–6642.
- (33) Schmitz, G.; Furrow, S. D. Kinetics of the iodate reduction by hydrogen peroxide and relation with the Briggs–Rauscher and Bray–Liebhafsky oscillating reactions. *Phys. Chem. Chem. Phys.* **2012**, *14*, 5711–5717.
- (34) Noszticzius, Z.; Noszticzius, E.; Schelly, Z. A. On the Use of Ion-Selective Electrodes for Monitoring Oscillating Reactions 1. Potential Response of the Silver Halide Membrane Electrodes to Hypohalous acids. *J. Am. Chem. Soc.* **1982**, *104*, 6194–6199.
- (35) Noszticzius, Z.; Noszticzius, E.; Schelly, Z. A. Use of Ion-Selective Electrodes for Monitoring Oscillating Reactions. 2. Potential Response of Bromide- Iodide-Selective Electrodes in Slow Corrosive Processes. Disproportionation of Bromous and Iodous Acids. A Lotka–Volterra model for the Halate Driven Oscillators. *J. Phys. Chem.* **1983**, *87*, 510–524.
- (36) Schmitz, G. Iodine Oxidation by Hydrogen Peroxide in Acidic Solutions, Bray–Liebhafsky Reaction and Other Related Reactions. *Phys. Chem. Chem. Phys.* **2010**, *12*, 6605–6615.
- (37) Hall, D. G. Ion-Selective Membrane Electrodes: A General Limiting Treatment of Interference Effects. *J. Phys. Chem.* **1996**, *100*, 7230–7236.
- (38) Masson, I. Hypoiodous Cations, and their Action upon an Organic Reagent. *J. Chem. Soc.* **1938**, 1708–1712.
- (39) Leden, I. On the Complexity of Cadmium and Silver Sulphate. *Acta Chem. Scand.* **1952**, *6*, 971–987.
- (40) Furrow, S. D. Reactions of Iodine Intermediates in Iodate–Hydrogen Peroxide Oscillators. *J. Phys. Chem.* **1987**, *91*, 2129–2135.
- (41) Schmitz, G.; Furrow, S. D. Kinetics of Iodous Acid Disproportionation. *Int. J. Chem. Kinet.* **2013**, *45*, 525–530.